

WFPC2 Re-Commissioning After Servicing Mission 3B

Anton M. Koekemoer, Shireen Gonzaga, Inge Heyer, Lori M. Lubin, Vera Kozhurina-Platais, and Brad Whitmore

Space Telescope Science Institute, 3700 San Martin Drive, Baltimore, MD 21218

Abstract. We describe here the results from an extensive series of tests and observations that we carried out with WFPC2 as part of the Observatory Verification program during March to April 2002, after SM3B. These tests included UV monitoring of possible contamination, performance checks of the biases, darks and other internal calibrations, as well as PSF and flatfield verification. The results from these tests show that there are no significant changes in the characteristics of the camera with respect to its pre-SM3B performance.

1. Introduction

In March 2002 Servicing Mission 3B (SM3B) was carried out, which included the addition of the NICMOS Cryo-cooler System (NCS) and the Advanced Camera for Surveys (ACS). While these will facilitate a wide range of science programs, WFPC2 retains a number of unique scientific capabilities. Thus, the WFPC2 SM3B plan involved protecting the health and safety of WFPC2 during and immediately after SM3B, and evaluating possible changes in its performance. Throughout SM3B and the subsequent 12 days of Bright-Earth Avoidance (BEA), WFPC2 was maintained in an inactive Protect Decon mode with the camera heads warm (+22° C), the shutter closed and the F785LP filter in place, to minimize the risk of potential contaminants entering the instrument and depositing on the optical surfaces. On March 23 2002, WFPC2 was cooled down to its nominal operating temperature of -88° C, and an extensive four-week program of Servicing Mission Orbital Verification (SMOV3B) calibration observations were commenced, to verify that the camera performance and characteristics remained essentially unchanged. Here we describe the analysis and results from these programs.

2. UV Contamination Monitoring

A critical component of WFPC2 cool-down involved intensive monitoring of the UV throughput, to ensure no permanent degradation by contamination deposited on the cold (-88° C) CCD windows. We began monitoring the standard star GRW+70d5824 immediately after cool-down, using the F170W filter in all four chips, repeated at 3, 6, 12, 18, 24, 36 hours, and 2, 3, 4, 5, 6 days after cooldown, after which a Decon was scheduled. UV observations were also obtained before and after each subsequent Decon during SMOV.

The results are presented in Figure 1, and can be summarized as follows: (1) at no point did any of the cameras exceed a 10% drop in throughput, well removed from the 30% limit; (2) the daily contamination rate was slightly higher than normal, but still below those during previous servicing missions; (3) the SMOV3B Decons successfully restored the F170W UV throughput to its nominal value; (4) the daily contamination rates now appear to have returned to their nominal values. Thus we conclude that our program of delayed cooldown, pro-active UV monitoring, and frequent decontaminations during SMOV3B were successful in fully retaining the F170W UV throughput capabilities of WFPC2.

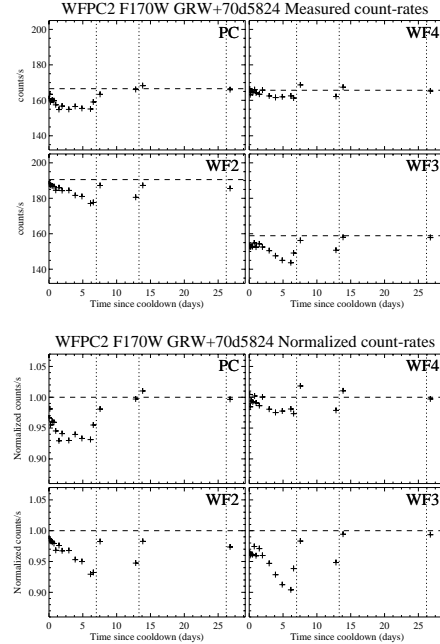


Figure 1. Measured decrease in the observed count-rate of GRW+70d5824 during the first month after cooldown, plotted for each of the cameras separately. The top panels show the measured count-rates, while the bottom panels show count-rates normalized to the pre-SMOV3B values. It can be seen that after each decon, the throughput is effectively returned to its nominal value.

3. Lyman- α Monitoring

During a servicing mission, contaminants could potentially settle on the WFPC2 pick-off mirror which is exposed to the *HST* hub area. We used F122M F160BW, by themselves and crossed with F130LP, to monitor the far-UV Lyman- α throughput for any decrease due to such contaminants. We used the historical GRW+70d5824 data to compare the contamination rate, and calculated the red-leak-corrected F122M data by subtracting the count rate measured in F122M+F130LP from that measured in the single F122M filter.

We find that all the data taken in F160BW and F160BW+F130LP are within 2 sigma of the mean value. For the F122M filter, the SMOV3B count rates are lower than the average value by 2–3 sigma, but this is in agreement with the historical long-term CTE degradation. The observed deviations in the red-leak-corrected F122M data are also consistent with those found after the previous two Servicing Missions. Thus, we conclude that the Lyman- α throughput shows no significant contamination as a direct result of SM3B.

4. Photometric Verification

This check was aimed at verifying the photometric accuracy to levels of 1 – 2%. The standard star GRW+70d5824 was observed in F160BW, F170W, F185W, F218W, F255W, F300W, F336W, F439W, F555W, F675W, and F814W, in all 4 CCDs. For each filter and CCD, we first fitted the long-term evolution of the photometric measurements, to account for CTE. We then expressed the post-SM3B measurements for each filter as a difference from the mean fitted trend, in units of the standard deviation of the historical data.

Figure 2 shows the statistical distribution of the post-SM3B measurements, normalized by the 1-sigma error for each filter. The distribution has a mean of 0.34 ± 0.26 sigma, thus

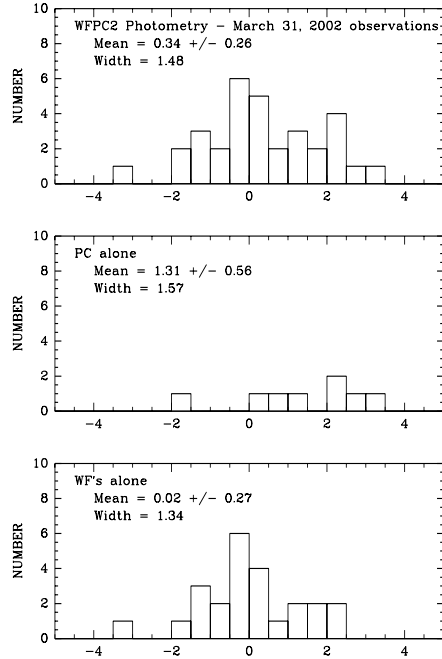


Figure 2. Statistical distribution of the post-SM3B photometry data points around the predicted values based on the fits obtained for each filter independently, and normalized by the 1-sigma error bars for each filter.

there is no obvious change in the throughput across SM3B. Since none of the filters deviate strongly from the mean, we conclude that the response of WFPC2 is essentially unchanged by SM3B, and that the long-term throughput decline is entirely consistent with the expected CTE loss.

5. Flat Field Verification

We examined observations of the bright Earth (“Earthflats”) to test the flat field stability and to verify that there is no unexpected OTA obscuration. We began with 124 pre-SM3B Earthflats in F502N, selected those obtained within 7 days after a Decon, and discarded images with mean PC1 counts < 500 DN and mean WF counts > 3200 DN, and with bad streaks. The remaining images were combined with the task *streakflat* to produce a pre-SM3B flat. A post-SM3B flat was created similarly, and divided by the pre-SM3B flat.

The only changes are on large scales at levels below 0.1–0.2%, well characterized based on long-term evolution of the camera vignetting (Koekemoer et al. 2002). Other evidence of small on-going geometric changes is seen in KSPOT images (Casertano and Wiggs 2001). The pixel-to-pixel fluctuations (over the central 400 x 400 pixels) in the ratio image are $\sim 0.4\%$ r.m.s. for the WFC CCDs and 0.8% r.m.s. for PC1, entirely consistent with photon noise. No change in chip-to-chip sensitivity is seen in on any levels above $\sim 0.3\%$, and there is no evidence of obscuration or other changes in the OTA. Thus we conclude that there are no significant changes in the flat fields due to SM3B.

6. PSF Monitoring

Following the procedures used after the previous two servicing missions (see Biretta et al. 1997; Casertano et al. 2000), images of Omega Cen were obtained to characterize the PSF.

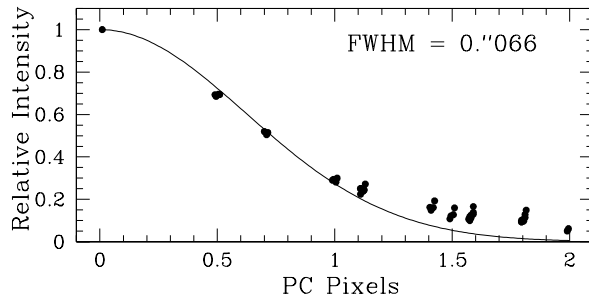


Figure 3. Radial profile of the PSF in the central region of the WFPC2 PC image of Omega Cen taken after SM3B. A composite stellar image was created using about 30 isolated, unsaturated stars near the chip center with the IRAF task *psf*, and the radial profile measured using the task *radprof*. The solid line shows the best-fit Gaussian model with $\text{FWHM}=0.''066$, comparing well with the pre-SM3B value of $0.''064$.

Four dithered images were obtained in F555W and F814W, sub-stepped by one-third of a pixel to provide a critically sampled PSF. The images were combined using the *dither* package. We used the task *psf* to construct a two-dimensional composite PSF from about 30 bright, unsaturated, isolated stars across the PC chip.

We then used the IRAF task *radprof* to measure the radial profile of the composite PSF (see Figure 3). The best-fit Gaussian has a FWHM of $0.''066 \pm 0.''002$, which compares well with the pre-SM3B value of $0.''064$ (Biretta et al. 1997; Casertano et al. 2000). We also measured the composite PSF across the rest of the chip. As previously noted (Krist & Burrows 1995), the off-center PSFs are more asymmetric due to coma and astigmatism. We find that this behavior is unchanged in our current measurements. Therefore we conclude that there are no significant changes in the WFPC2 PSF after SM3B.

7. Internal Monitoring

The internal monitoring observations for program 8950 were commenced immediately after cooldown, repeated regularly throughout SMOV3B, and included biases, dark frames, INTFLATs, VISFLATS, and Kellsall-spot (KSPOT) images.

The bias frames were used to determine the read-out noise, using the 16 bias frames obtained after SM3B, and comparing with a similar number from before SM3B (Figure 4). The dark current was measured using 40 darks obtained after SM3B and the same number obtained before. No changes are evident to levels below 0.1 – 0.2 DN. We used the 16 post-SM3B INTFLATs to compare with a similar pre-SM3B dataset, and found no changes above $\sim 0.5\%$, all consistent with well-documented small long-term changes in the INTFLAT lamp. We also compared VISFLATS from before and after SM3B and found that the gain ratios of all the chips remained constant to within 1%. Finally, we obtained 16 KSPOT images during SMOV3B, and compared these with a similar pre-SM3B dataset. We found that the spot locations for each chip agree to within a few mas, fully consistent with the slow long-term evolution previously discussed by Casertano and Wiggs (2001).

8. Summary

Overall, WFPC2 appears to be very stable, exhibiting only the minor changes expected due to known long-term evolution, and there are no significant changes attributable to SM3B.

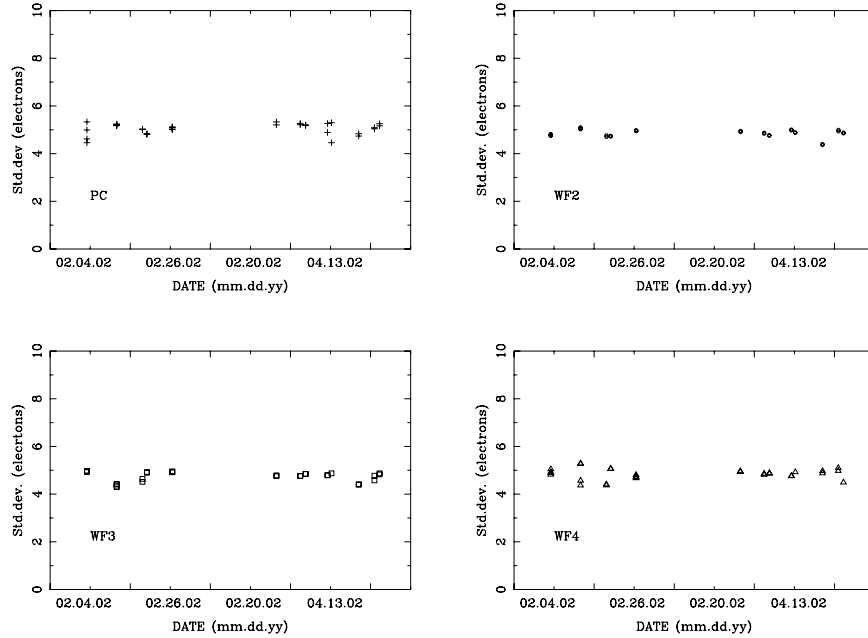


Figure 4. Comparison of the r.m.s. read-noise measured from bias frames taken before and after SM3B, for the four WFPC2 chips (PC, WF2, WF3, WF4), at gain=7. There is no significant change at all in the read-noise for any of the chips, at either gain=7 or 15.

References

- Biretta, J., et al. 1997, *Instrument Science Report WFPC2-97-09* (Baltimore: STScI)
- Casertano, S., et al. 2000, *Instrument Science Report WFPC2-00-02* (Baltimore: STScI)
- Casertano, S. & Wiggs, M. 2001, *Instrument Science Report WFPC2-01-10* (Baltimore: STScI)
- Koekemoer, A. M., Biretta, J., & Mack, J., 2002, *Instrument Science Report WFPC2-02-02* (Baltimore: STScI)
- Koekemoer, A. M., Gonzaga, S., Lubin, L., Whitmore, B., & Heyer, I., 2002, *Technical Instrument Report WFPC2-02-03* (Baltimore: STScI)
- Koekemoer, A. M., et al. 2002, *HST Dither Handbook, Version 2.0* (Baltimore: STScI)
- Krist, J. & Burrows, C. 1995, *Applied Optics* 34, 4952
- Lubin, L. M., Whitmore, B., Koekemoer, A. M., & Heyer, I. 2002, *Technical Instrument Report WFPC2-02-05* (Baltimore: STScI)